From networks of unstable attractors to heteroclinic switching

Christoph Kirst[1,2,3,4] and Marc Timme[1,2]

[1]*Network Dynamics Group, Max Planck Institute for Dynamics and Self-Organization (MPIDS), 37073 Göttingen, Germany*
[2]*Bernstein Center for Computational Neuroscience (BCCN) Göttingen, 37073 Göttingen, Germany*
[3]*Fakultät für Physik, Georg-August-Universität Göttingen, Germany*
[4]*DAMPT, Centre for Mathematical Sciences, Cambridge University, Cambridge CB3 0WA, United Kingdom*

We present a dynamical system that naturally exhibits two unstable attractors that are completely enclosed by each other's basin volume. This counterintuitive phenomenon occurs in networks of pulse-coupled oscillators with delayed interactions. We analytically show that upon continuously removing a local noninvertibility of the system, the two unstable attractors become a set of two nonattracting saddle states that are heteroclinically connected. This transition equally occurs from larger networks of unstable attractors to heteroclinic structures and constitutes a new type of singular bifurcation in dynamical systems.

The concepts of attractor and stability are at the core of dynamical systems theory [1] because attractivity and stability determine the long-term behavior and often the typical properties of a system. Attraction and stability which may change via bifurcations are thus fundamental to modeling in all of science and engineering. For systems with smooth and invertible flows these concepts have long been studied and are well understood, allowing classifications of dynamical systems and their bifurcations, for example, by using topological equivalence and normal forms.

Dynamical systems with nonsmooth or noninvertible flows, such as hybrid or Fillipov systems [2], are far less understood, although they model a variety of natural phenomena, ranging from the mechanics of stick-slip motion and the switching dynamics of electrical circuits to the generation of earthquakes and the spiking activity of neural networks [3–5]. For instance, spiking neurons interact by sending and receiving electrical pulses at discrete instances of time, which interrupt the intermediate smooth interaction-free dynamics. This neural dynamics and similarly that of, e.g., cardiac pacemaker cells, plate tectonics in earthquakes, chirping crickets, and flashing fireflies are often modeled as pulse-coupled oscillators.

Such hybrid systems display dynamics very different from that of temporally continuous or temporally discrete systems. Networks of oscillators with global homogeneous delayed pulse-coupling may robustly exhibit *unstable attractors* [5] (invariant periodic orbits that are Milnor attractors [1], but locally unstable). In the presence of noise, these systems exhibit a dynamics akin to heteroclinic switching [6], a feature that is functionally relevant in many natural systems such as in neural, weather, and population dynamics [6,7]. Rigorous analysis [8] shows that invertible systems in general cannot have unstable attractors and that a saddle state can in principle be converted to an unstable attractor by locally adding a noninvertible dynamics onto the stable manifold. However, the potential relation of unstable attractors to heteroclinic cycles is not well understood and it is unknown whether and how unstable attractors may be created or destroyed via bifurcations.

In a network of pulse-coupled oscillators we here demonstrate the existence of two unstable attractors that are enclosed by the basin of attraction of each other. We explain this counterintuitive phenomenon: Continuously lifting the local noninvertibility of the system with two unstable attractors creates a standard heteroclinic two-cycle. This transition equally occurs from large networks of unstable attractors to heteroclinic structures and constitutes a new type of singular bifurcation in hybrid dynamical systems.

We consider a network of N oscillatory units with a state defined by a phaselike variable $\phi_i(t) \in \mathbb{R}$, $i \in \{1, 2, \dots, N\}$, which increases uniformly in time t:

$$\frac{d}{dt}\phi_i = 1. \tag{1}$$

Upon crossing a threshold at time t_s, $\phi_i(t_s) \geq 1$, unit i is instantaneously reset:

$$\phi_i(t_s^+) := \lim_{r \searrow 0} \phi_i(t_s + r) = K(\phi_i(t_s)). \tag{2}$$

Here $K(\phi) = U^{-1}(R(U(\phi)-1))$ is determined by a smooth, unbounded, strictly monotonic increasing *rise function* $U(\phi)$ normalized to $U(0)=0$ and $U(1)=1$ and a smooth nonnegative *reset function* R satisfying $R(0)=0$. In addition to the reset (2) a pulse is sent which is received by all units j after a delay time $\tau > 0$, inducing a phase jump

$$\phi_j(t_s + \tau) = H_{\varepsilon_{ji}}(\phi_j((t_s + \tau)^-)), \tag{3}$$

with *interaction function* $H_\varepsilon(\phi) = U^{-1}(U(\phi)+\varepsilon)$ and coupling strength ε_{ji} from unit i to unit j. We set $J_\varepsilon(\phi) = K \circ H_\varepsilon(\phi)$ and denote a phase shift by $S_\eta(\phi) = \phi + \eta$.

This system represents, for instance, an abstract model of neuronal oscillators with a membrane potential $u_i(t) = U(\phi_i(t))$. The neurons' responses to synaptic inputs are described by increasing the potentials instantaneously by an amount ε_{ij}, which represents the transferred charge from the pulse-sending (presynaptic) neuron j to the pulse-receiving (postsynaptic) one i. If this input is suprathreshold, $u_i(t) = u_i(t^-) + \varepsilon_{ij} > 1$, unit i is *partially reset* to
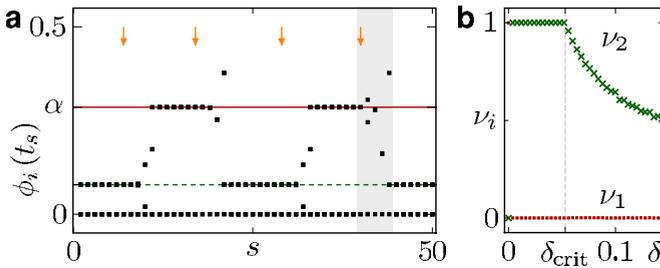
FIG. 1. (Color online) Two unstable attractors enclosed by the basins of each other ($c=0$). (a) Phases $\phi_i(t_s)$ (dots) of all units at times t_s just after the sth reset of a reference unit $i=1$. Lines indicate the phases on the invariant orbit A_1 (α, solid line) and A_2 (dashed line). Arrows mark times of small phase perturbations which induce switches from A_1 to A_2 or vice versa. The shaded area highlights a switch from A_1 to A_2 that is shown in detail in Fig. 2. (b) Fraction ν_i of 5000 trajectories reaching the periodic orbit A_i (■: $i=1$; ×: $i=2$) starting from random phases distributed uniformly in a box of side width 2δ centered around $\phi=a_1$ on the orbit A_1. For $0<\delta<\delta_{\mathrm{crit}}\approx0.05$ all trajectories reach the orbit A_2 ($\nu_2=1$), indicating that A_1 is enclosed by the basin volume of A_2 and in particular that A_1 is an unstable attractor.

$$u_i(t^+) = R(u_i(t) - 1) \geqslant 0. \qquad (4)$$

This accounts for remaining synaptic input charges which are not used to reach the threshold and which contribute to the potential after reset [9]. For $R(\zeta)\equiv0$ we recover the model analyzed in previous studies [5], which has a local noninvertibility since the original phase of a unit cannot be recovered after it received suprathreshold input and was reset to $J_\varepsilon(\phi)\equiv0$. For an invertible R the flow becomes locally time invertible.

Here we focus on a homogeneous network of all-to-all coupled excitatory units without self-interaction—i.e., $\varepsilon_{ij}=(1-\delta_{ij})\varepsilon$, $\varepsilon>0$. The permutation symmetry implies invariant subspaces of two or more synchronized units and thus the possibility of robust heteroclinic cycles; cf. [10]. For the numerical simulations presented below, we fix $\varepsilon=0.23$, $\tau=0.02$, a rise function $U(\phi)=\frac{1}{b}\log(1+[\exp(b)-1]\phi)$ with $b=4.2$, and partial reset $R(\zeta)=c\zeta$ with parameter $c\in[0,1]$, which is invertible for all $c>0$. For these parameters the model exhibits short switching times between periodic orbits, which simplifies the presentation of the analysis below; however, the studied phenomena are robust against structural perturbations in τ, ε, and the function U.

For locally noninvertible dynamics ($c=0$) the above system exhibits unstable attractors in a large fraction of parameter space and for different network sizes N [5,8]. For the above parameters, the smallest system in which we observed unstable attractors has $N=4$ units. Curiously, numerical simulations [e.g., Fig. 1(a)] indicate that such a system exhibits two unstable attractors, each of which is fully enclosed by the basin volume of the other attractor [Fig. 1(b)].

We confirm these numerical findings analytically. Given a periodic orbit A, define the basin of attraction $\mathcal{B}(A)$ as the set of points in state space that converge to A in the long-time limit. Below we show that in the system (1)–(3) with $R(\zeta)\equiv0$ there is a pair of periodic orbits A_1 and A_2 such that a

full measure set of points of an open neighborhood of A_1 is contained in the basin $\mathcal{B}(A_2)$ and vice versa.

To study the dynamics in detail we use an event-based analysis; cf. e.g., [4]. The event when a unit i sends a pulse is denoted by s_i, the reception of a pulse from unit j by r_j, and simultaneous events are enclosed in parentheses. For a given parameter $c\in[0,1]$, a simple saddle periodic orbit A_1 [cf. Figs. 1(a) and 3(a)] is uniquely determined by the cyclic event sequence

$$E(A_1) = (s_1,s_2)(r_1,r_2,s_3,s_4)(r_3,r_4). \qquad (5)$$

By exchanging the indices $(1,2)\leftrightarrow(3,4)$ in (5) we obtain the event sequence of a permutation-equivalent periodic orbit A_2. Both orbits lie in the intersection of the two invariant subspaces $\{\phi_1=\phi_2\}$ and $\{\phi_3=\phi_4\}$ with synchronized units (1, 2) and (3, 4), respectively. This allows a robust heteroclinic connection between them [10]. As it turns out below, the local stability and nonlocal attractivity properties of the A_i depend on the parameter c.

We now first locally reduce the infinite-dimensional state space of the hybrid dynamical system with delayed coupling to three dimensions: Local to A_1 and A_2 the state space reduces in finite time [8] to an eight-dimensional state space spanned by the four phases $\phi=(\phi_1,\phi_2,\phi_3,\phi_4)$ and the four times $\sigma_i\geqslant0$, $i\in\{1,\dots,4\}$, elapsed since the most recent pulse generation of oscillator i. We consider the subset $\mathcal{M}=\{(\phi,\sigma)\,|\,\sigma_i>\tau,i\in\{1,\dots,4\}\}$ of the state space where all pulses have been received: Then the state space is effectively four dimensional, since the exact values of the $\sigma_i>\tau$ do not influence the dynamics. Due to the uniform phase shift (1), A_1 is a straight line in $\mathcal{M}$ after the last and before the first event in the sequence (5). We denote the point in the center of this line by a_1 and consider states with phases $\phi=a_1+(\delta_1,\delta_2,\delta_3,\delta_4)$ in a neighborhood. Because of shift invariance, we may further fix $\delta_1=0$, being left with a locally three-dimensional representation $\mathcal{P}_1\subset\mathbb{R}^3$ of the original state space with states $(\delta_2,\delta_3,\delta_4)\in\mathcal{P}_1$. Similarly, we have a local three-dimensional representation $(\delta_4,\delta_1,\delta_2)\in\mathcal{P}_2$ of the state space around $a_2\in\mathcal{M}\cap A_2$, constructed analogously to a_1, this time fixing $\delta_3=0$. There is an open neighborhood of A_i in the full eight-dimensional state space from which every orbit crosses $\mathcal{P}_i$ after at most eight events (one cycle). In this sense $\mathcal{P}_i$ is a three-dimensional Poincaré section in a neighborhood of A_i.

For arbitrary $c\in[0,1]$ there are regions in $\mathcal{P}_1$ and $\mathcal{P}_2$ from which all trajectories evolve back to points in either $\mathcal{P}_1$ or $\mathcal{P}_2$. Between these regions we derive return maps and their domains which follow directly from the definition of the local state space and the event sequence (Fig. 2 visualizes domains of the key maps and a sample trajectory for $c=0$). For instance, the orbit A_1 is enclosed by the three-dimensional domain $\mathcal{C}_1\subset\mathcal{P}_1$ of the return map $F:\mathcal{C}_1\to\mathcal{P}_1$,

$$F(\delta_2,\delta_3,\delta_4) = (\mathrm{sgn}(\delta_2)[H_{2\varepsilon}\circ S_\tau\circ H_\varepsilon(\tau+|\delta_2|)$$
$$- H_{2\varepsilon}\circ S_{\tau+|\delta_2|}\circ H_\varepsilon(\tau-|\delta_2|)], \delta_3', \delta_4'), \qquad (6)$$

which is determined by the event sequence
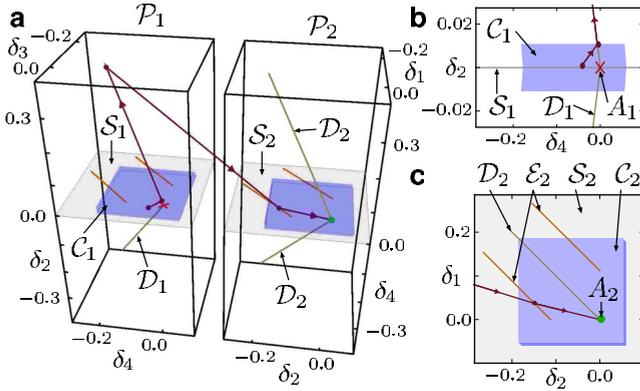
FIG. 2. (Color online) Structure of the three-dimensional re-duced state space for $c=0$ showing that the A_i are unstable attractors enclosed by the basins of each other. (a) Representations $\mathcal{P}_i$ of the state space in a neighborhood of $A_1 \in \mathcal{P}_1$ (cross) and $A_2 \in \mathcal{P}_2$ (ball). All trajectories starting in the set $\mathcal{C}_1$ (close to A_1) lead to a switch to A_2. The line with arrows shows a sample trajectory of the marked switch from A_1 to A_2 in Fig. 1(a). (b) Projection of $\mathcal{P}_1$ onto the δ_2-δ_4 plane and (c) of $\mathcal{P}_2$ onto the δ_1-δ_2 plane, illustrating that, except for the lower-dimensional subset $\mathcal{S}_i$, the attractor A_i is en-closed by $\mathcal{C}_i$; i.e., the A_i are unstable attractors.

$$E(\mathcal{C}_1) = (s_1)(s_2)(r_1)(r_2,s_3,s_4)(r_3,r_4) \qquad (7)$$

or its equivalent with permuted indices $1 \leftrightarrow 2$. Here

$$\delta_i' = H_\varepsilon \circ S_\tau \circ J_\varepsilon(H_\varepsilon(\alpha + \tau + \delta_i) + |\delta_2|) + 1$$
$$- H_{2\varepsilon} \circ S_\tau \circ H_\varepsilon(\tau + |\delta_2|) - \alpha \qquad (8)$$

for $i \in \{3,4\}$, where the phase difference α between the two synchronized clusters at a_1 is determined by

$$\alpha = H_\varepsilon \circ S_\tau \circ J_{2\varepsilon}(\alpha + \tau) + 1 - H_{2\varepsilon} \circ S_\tau \circ H_\varepsilon(\tau). \qquad (9)$$

For $|\delta_2| > 0$, F is expanding in the δ_2 direction since

$$|(F(\delta))_2| > k|\delta_2|, \qquad (10)$$

with $k = \min_{\phi \in [0,1]} H_\varepsilon(\phi) > 1$. For $\delta_2 = 0$ we obtain a map with the same explicit form as in (6), but with event se-quence as in (5), whose domain is a subset of the two-dimensional invariant set $\mathcal{S}_1 = \{\delta \in \mathcal{P}_1 | \delta_2 = 0\}$, where units 1 and 2 are synchronized. States in $\mathcal{S}_1$ converge to A_1 in the long-time limit. Similarly, points in $\mathcal{S}_2 = \{\delta \in \mathcal{P}_2 | \delta_4 = 0\}$ reach A_2 asymptotically.

If the system is locally noninvertible ($c=0$), the dynamics is as follows (see Fig. 2): Since $J_\varepsilon(\phi) \equiv 0$, $\delta_3' = \delta_4'$ according to (8) and hence F maps $\mathcal{C}_1$ to two one-dimensional lines $\mathcal{D}_1 = F(\mathcal{C}_1)$. Since F is expanding in δ_2, expression (10), all points in $\mathcal{D}_1 \cap \mathcal{C}_1$ are mapped after a finite number of inter-actions to $\mathcal{D}_1 \backslash \mathcal{C}_1$. The set $\mathcal{D}_1 \backslash \mathcal{C}_1$ is mapped to $\mathcal{E}_2 \subset \mathcal{S}_2$ and from there to the attractor A_2. In Fig. 2 we have plotted a sample trajectory for the switch marked in Fig. 1(a). For the positive measure set $\mathcal{C}_1 \cup \mathcal{S}_1$, which encloses A_1, we thus have $\mathcal{C}_1 \subset \mathcal{B}(A_2)$ and only the zero-measure subset $\mathcal{S}_1$ con-verges to A_1. Thus A_1 is an unstable attractor. Permutation symmetry implies analogous dynamics near A_2. Taken to-gether, for $c=0$ the periodic orbits A_1 and A_2 are unstable attractors enclosed by the basins of each other.
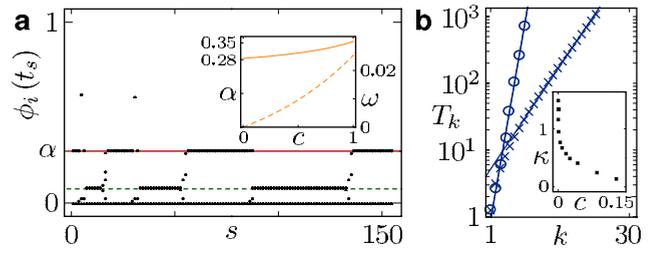
FIG. 3. (Color online) Heteroclinic switching ($c>0$). (a) Phases $\phi_i(t_s)$ (dots) as in Fig. 1(a) for $c=0.05$. The invariant periodic orbits A_i, being unstable attractors at $c=0$, still exist for $c>0$ (solid and dashed lines). Starting in a state near A_1 leads to repeated switching between the two states. Inset: phase difference α (9) (solid line) and side width w of the set $\mathcal{D}_i'$, Eq. (11) (dashed line), change continu-ously upon increasing c from zero. (b) Switching times T_k up to the kth switch ($\times$: $c=0.1$; $\circ$: $c=0.01$) increase exponentially with k, indicating that the dynamics evolve near a heteroclinic cycle be-tween the invariant states. Inset: fitting $T_k = \gamma e^{\kappa k}$ to the switching times for several values of c we find a divergence of κ as $c \to 0$.

If we remove the local noninvertibility ($c>0$), the dy-namics changes qualitatively as shown in Fig. 3: The two periodic orbits A_i with event sequence (5) still exist; only the phase difference α changes continuously with c [Fig. 3(a)]. Starting in a state close to one of the A_i leads to trajectories with switching between both of them. The switching time increases exponentially with the number of switches [Fig. 3(b)], indicating that these dynamics originate from an orbit near a heteroclinic two-cycle. Furthermore, the switching times diverge as $c \to 0$ [cf. Fig. 3(b)], suggesting the transi-tion to a network of unstable attractors at $c=0$. Indeed, the structure of the domains of all return maps does not change qualitatively when c increases from zero. However, since J_ε becomes invertible for $c>0$, according to (8) a phase differ-ence $|\delta_3 - \delta_4|$ shrinks under the return map F, but does not collapse to zero as for $c=0$; hence, the image $\mathcal{D}_1' = F(\mathcal{C}_1)$ stays three dimensional. It consists of tubes (around the original lines $\mathcal{D}_1$) with a square cross section of side width

$$w(c) = H_\varepsilon \circ S_\tau \circ U^{-1}(c\varepsilon) - H_\varepsilon \circ S_\tau \circ U^{-1}(0), \qquad (11)$$

which continuously increases with c from $w(0)=0$ [Fig. 3(a)]. This reflects the local c-dependent contraction of the state space according to (6) and (8). All maps with domains that have a nonempty intersection with $\mathcal{D}_1'$ map $\mathcal{D}_1'$ to a three-dimensional state-space volume around A_2 that is a subset of $\mathcal{C}_2 \cup \mathcal{S}_2$. Taken together, states in the three-dimensional set $\mathcal{C}_1$ evolve to states in a positive measure subset of $\mathcal{C}_2 \cup \mathcal{S}_2$ that encloses A_2. Using symmetry again, $\mathcal{C}_2$ is analogously mapped to a subset of $\mathcal{C}_1 \cup \mathcal{S}_1$. This explains the observed switching.

The unstable attractors are converted to nonattracting saddles by removing the local noninvertibility of the dynam-ics, which is reflected by the expansion of $\mathcal{D}_i$, $i \in \{1,2\}$, to positive measure sets $\mathcal{D}_i'$ when increasing c from zero. More-over, states in the subset of $\mathcal{C}_1$ with synchronized units 3 and 4—i.e., states in the set $\{\delta \in \mathcal{C}_1 | \delta_3 = \delta_4\}$—are mapped to $\mathcal{S}_2$ and thus reach the orbit A_2 asymptotically. Hence, this set together with all its image points in $\mathcal{P}_1$ and $\mathcal{P}_2$ forms a het-

eroclinic connection from A_1 to A_2. Thus, by symmetry, the network of two unstable attractors ($c=0$) continuously bifurcates to a heteroclinic two-cycle ($c>0$).

The underlying mechanism relies on the interplay of the local instability (10) and the parameter-dependent contraction induced by the reset (4), implying the same transition in larger systems (not shown). For locally noninvertible dynamics these display larger networks of unstable attractors [5] with a link between two attractors $A_i \rightarrow A_j$ if every neighborhood of A_i contains a positive basin volume of A_j. Upon lifting the local noninvertibility each link in this network is replaced by a heteroclinic connection.

In summary, we have presented and analyzed the counterintuitive phenomenon of two unstable attractors that are enclosed by each other's basin volume. We explained this phenomenon by showing that there is a continuous transition from two unstable attractors to a heteroclinic two-cycle. Larger networks of unstable attractors equally show this transition to more complex heteroclinic structures. It constitutes a new type of singular bifurcation in dynamical systems and establishes the first known bifurcation of unstable attractors. Moreover, our results show that this bifurcation occurs upon continuously removing the noninvertibility of the system, whereas both the noninvertible ($c=0$) and the locally invert-ible ($c>0$) systems exhibit equally discontinuous interactions. This explicitly demonstrates that the local noninvertibility and not the discontinuity is responsible for the creation of unstable attractors [8].

The continuity of the bifurcation has theoretical and practical consequences: For instance, one may investigate features of a system exhibiting heteroclinic switching [6] by studying its limiting counterpart with unstable attractors. Furthermore, this may help designing systems with specific heteroclinic structure, for instance in artificial neural networks, and guide our understanding of time series of switching phenomena in nature; cf. [7]. The associated limiting systems with unstable attractors may not only be analytically accessible, also numerical simulations can be performed in a more controlled way because typical problems with simulations of heteroclinic switching (e.g., exponentially increasing switching times and exponentially decreasing distances to saddles) do not occur if the heteroclinic switching is replaced by networks of unstable attractors.

[1] A. Katok and B. Hasselblatt, *Introduction to the Modern Theory of Dynamical Systems* (Cambridge University Press, Cambridge, England, 1995); J. Milnor, Commun. Math. Phys. **99**, 177 (1985).

[2] B. Brogliato, *Nonsmooth Mechanics* (Springer, Berlin, 1999); M. di Bernardo *et al.*, *Piecewise-Smooth Dynamical Systems* (Springer, Berlin, 2007).

[3] Z. Olami, H. J. S. Feder, and K. Christensen, Phys. Rev. Lett. **68**, 1244 (1992); J. H. B. Deane and D. C. Hamill, IEEE Trans. Power Electron. **5**, 260 (1990); R. E. Mirollo and S. H. Strogatz, SIAM J. Appl. Math. **50**, 1645 (1990); A. V. M. Herz and J. J. Hopfield, Phys. Rev. Lett. **75**, 1222 (1995); W. Senn and R. Urbanczik, SIAM J. Appl. Math. **61**, 1143 (2001).

[4] M. Timme, F. Wolf, and T. Geisel, Phys. Rev. Lett. **89**, 258701 (2002).

[5] U. Ernst, K. Pawelzik, and T. Geisel, Phys. Rev. Lett. **74**, 1570 (1995); Phys. Rev. E **57**, 2150 (1998); M. Timme, F. Wolf, and T. Geisel, Phys. Rev. Lett. **89**, 154105 (2002); Chaos **13**, 377 (2003).

[6] J. H. P. Dawes and T. L. Tsai, Phys. Rev. E **74**, 055201(R) (2006); C. M. Postlethwaite and J. H. P. Dawes, Nonlinearity **18**, 1477 (2005); R. M. May and W. J. Leonard, SIAM J. Appl. Math. **29**, 243 (1975); D. Hansel, G. Mato, and C. Meunier, Phys. Rev. E **48**, 3470 (1993); H. Kori and Y. Kuramoto, *ibid.* **63**, 046214 (2001); P. Ashwin and J. Borresen, *ibid.* **70**, 026203 (2004); P. Ashwin, O. Burylko, Y. Maistrenko, and O. Popovych, Phys. Rev. Lett. **96**, 054102 (2006).

[7] P. Ashwin and M. Timme, Nature (London) **436**, 36 (2005).

[8] P. Ashwin and M. Timme, Nonlinearity **18**, 2035 (2005).

[9] C. Kirst, T. Geisel, and M. Timme, e-print arXiv:0810.2749v1.

[10] M. Krupa, J. Nonlinear Sci. **7**, 129 (1997).